Effect of coupling point selection on distortion in internet-distributed hardware-in-the-loop simulation

Tulga Ersal and R. Brent Gillespie

Department of Mechanical Engineering,
University of Michigan,
2350 Hayward St.,
Ann Arbor, MI 48109, USA
E-mail: tersal@umich.edu
E-mail: brentg@umich.edu

Mark J. Brudnak

6501 E. 11 Mile Road,
Bldg. 215 (RDTA-RS) Room 45,
MS/157,Warren, MI 48397-5000, USA
E-mail: mark.j.brudnak.civ@mail.mil

Jeffrey L. Stein

Department of Mechanical Engineering,
University of Michigan,
2350 Hayward St., Ann Arbor, MI 48109, USA
E-mail: stein@umich.edu

Hosam K. Fathy*

The Pennsylvania State University,
157D Hammond Building,
University Park, PA 16802, USA
E-mail: hkf2@psu.edu
*Corresponding author

Abstract: The degree to which an Internet-Distributed Hardware-In-the-Loop (ID-HIL) simulation loses fidelity relative to the single-location alternative is referred to as distortion. This paper shows that, besides delay, the choice of coupling point, i.e., the port at which the system model is integrated across the Internet, also affects distortion. To quantify distortion, a frequency-domain metric is proposed using a linear systems framework. This metric is then used to analyse how the choice of coupling point affects distortion, leading to guidelines for selecting a coupling point that gives minimal distortion. The theory is demonstrated on a quarter-car model.

Keywords: coupling points; Internet-distributed hardware-in-the-loop simulation; ID-HILS; delay systems; distortion.

Biographical notes: Tulga Ersal received the BS degree from the Istanbul Technical University, Istanbul, Turkey, in 2001, and the MS and PhD degrees from the University of Michigan, Ann Arbor, MI, in 2003 and 2007, respectively, all in mechanical engineering. He is currently an Assistant Research Scientist in the Department of Mechanical Engineering, University of Michigan, Ann Arbor, MI. His research interests include modelling and control of dynamic systems, model order and structure reduction, multibody dynamics and integration of distributed hardware-in-the-loop systems.

R. Brent Gillespie received the BS degree in mechanical engineering from the University of California, Davis, in 1986, the MM degree in piano performance from the San Francisco Conservatory of Music in 1989, and the MS and PhD degrees in mechanical engineering from Stanford University, Stanford, CA, in 1992 and 1996, respectively. He is currently an Associate Professor in the Department of Mechanical Engineering, University of Michigan, Ann Arbor. His current research interests include haptic interface and teleoperator control, human motor control, and robot-assisted rehabilitation after neurological injury.

Mark Brudnak received his BS degree in electrical engineering from Lawrence Technological University, Southfield, Michigan in 1991, his MS degree in electrical and computer engineering and his PhD degree in systems engineering from Oakland University, Rochester, Michigan in 1996 and 2005, respectively. He is an Associate Director at the US Army Tank Automotive Research Development and Engineering Center (TARDEC), Warren, MI, which is a component of the Research Development and Engineering Command (RDECOM). In this capacity, he oversees the operation of laboratories for durability testing, vehicle characterisation and human-in-the-loop motion base simulation. His research interests include integration of distributed hardware-in-the-loop systems, the control and modelling black-box dynamical systems, support vector machines, machine learning, and multibody dynamics.

Jeffrey L. Stein received the BS degree in premedical studies from the University of Massachusetts, Amherst, MA, in 1973, and the SB, SM, and PhD degrees in mechanical engineering from the Massachusetts Institute of Technology, Cambridge, MA, in 1976, 1976, and 1983, respectively. Since 1983 he has been with the University of Michigan, Ann Arbor, MI, where he is currently a Professor of Mechanical Engineering. His research interests include computer based modelling and simulation tools for system design and control, with applications to vehicle-to-grid integration, vehicle electrification, conventional vehicles, machine tools, and lower leg prosthetics. He has particular interest in algorithms for automating the development of proper dynamic mathematical models, i.e., minimum yet sufficient complexity models with physical parameters.

Hosam K. Fathy received the PhD degrees from the University of Michigan, Ann Arbor, in 2003, the MS degree from Kansas State University, Manhattan, in 1999, and the BSc degree from the American University, Cairo, Egypt, in 1997, all in mechanical engineering. He is an Assistant Professor of Mechanical Engineering at the Pennsylvania State University, University Park, PA, since 2010. Prior to that, he was a Mechanical Engineering Research Scientist with the Department of Mechanical Engineering, University of

Michigan, Ann Arbor. His Control Optimisation Laboratory is active in the battery health, V2G power management, and ID-HIL simulation areas, with funds from NSF, DOE, and DOD. He has taught vehicle dynamics, engineering analysis, and battery modelling and control.

1 Introduction

Hardware-In-the-Loop Simulation (HILS) refers to simulating a system by coupling physical models of some of its components together with mathematical models of its remaining components (Bacic et al., 2009). Thus, it combines the high fidelity of physical prototyping with the cost effectiveness of model-based simulation (Fathy et al., 2006). It strongly promotes concurrent system engineering and has therefore become indispensable in many application areas, such as the automotive (Kimura and Maeda, 1996; Zhang and Alleyne, 2005; Verma et al., 2008), aerospace (Leitner, 2001; Yue et al., 2005; Cai et al., 2009), manufacturing (Ganguli et al., 2005), robotics (Aghili and Piedboeuf, 2002; White et al., 2009), and defence areas (Huber and Courtney, 1997; Buford et al., 2000).

To exploit the benefits of HILS fully, it may be desirable to integrate multiple HILS setups (Kelf, 2001). Recent efforts have focused on achieving such integration over the Internet to allow for integration of setups that are geographically dispersed and unfeasible to couple physically. For example, the George E. Brown Jr. Network for Earthquake Engineering Simulation (NEES) (Mahin et al., 2003) provides an outstanding example of the capabilities and impact of the ID-HILS idea, and the earthquake literature presents many other applications of the ID-HILS idea to earthquake simulation (Watanabe et al., 2001; Tsai et al., 2003; Spencer et al., 2004; Pan et al., 2005; Stojadinovic et al., 2006; Mosqueda et al., 2008). Another example in the automotive application area is the integration of a ride motion simulator in Warren, MI, USA, with a hybrid-powertrain-system simulator in Santa Clara, CA, USA (Compere et al., 2006; Goodell et al., 2006; Brudnak et al., 2007) and, as a separate effort, with an engine-in-the-loop simulator in Ann Arbor, MI, USA (Ersal et al., 2011). These efforts highlight the potential impact of ID-HILS for automotive systems.

Coupling HILS setups over the Internet introduces a deviation from the dynamics that would otherwise be observed if the setups were collocated and could be directly integrated. This deviation is termed distortion in the present paper.

There are several sources of distortion in an ID-HIL setup. Distributing a system into subsystems that are co-simulated using independent numerical solvers can be in and of itself an important source of distortion due to the lack of access to the Jacobians of the remote sites, sampling effects, etc., even without any delay (Ersal et al., 2012). Distribution over the Internet introduces further distortion due to the Internet's delay, jitter, and loss. Jitter refers to the variability of delay, and loss means that not all packets sent arrive at their destination. Recognising these issues, the literature has proposed methods to assess the relative impact of distribution effects in comparison to the effects of the Internet's delay, jitter, and loss (Ersal et al., 2012). The literature has also developed various approaches to address stability and distortion issues under a delayed coupling of subsystems, including passivity-based (Anderson and Spong, 1989;

Niemeyer and Slotine, 1991, 2002; Lee and Spong, 2006), event-based (Xi and Tarn, 2000; Elhajj et al., 2003; Mosqueda et al., 2008), and observer-based (Compere et al., 2006; Goodell et al., 2006; Brudnak et al., 2007; Wagg et al., 2008) frameworks. Furthermore, techniques to compensate for actuator delays and lags in HILS systems have been proposed (Horiuchi et al., 1999; Blakeborough et al., 2001; Darby et al., 2002; Wallace et al., 2005; Jung and Shing, 2006; Wagg et al., 2008), and linear control theory based methods have been developed to analyse and improve stability and stability robustness (Wagg et al., 2008).

This paper focuses on another potential variable that can affect distortion, namely, the coupling point. Within the context of this paper, the term 'coupling point' refers to the point at which the HILS system is divided into two subsystems that are then co-simulated. While options for placement of the coupling point may not always exist, when they do exit, the location of the coupling point can become a design parameter. Then, it becomes important to know how to best pick that design parameter to minimise distortion. Note that coupling points and their causality were previously considered in terms of their effect on stability (Gawthrop et al., 2009); however, the focus of this paper is their effect on distortion.

Thus, the aim of this paper is to develop a framework in which the impact of coupling point selection on distortion can be studied and the conditions that make one coupling point better than another can be understood. As a first step, this paper will consider only the effect of delay and ignore jitter, loss, and distributed simulation effects (numerical issues due to separate solvers, sampling effects, etc.,). This consideration is justified by the observation that it is easy to conceive an ID-HIL setup in which delay is the dominant cause of distortion and jitter, loss, and distributed simulation effects are negligible (Ersal et al., 2012). In addition, the paper will consider linear systems. These assumptions will not only simplify the problem, but also allow for the analysis to be handled through a deterministic, continuous, linear framework. Such a framework will, in turn, allow for leveraging the existing frequency-domain characterisations of distortion (Lawrence, 1993; Yokokohji and Yoshikawa, 1994; Çavuşoğlu et al., 2002; De Gersem et al., 2005; Griffiths et al., 2008).

The rest of the paper is organised as follows. A motivating example is given first in Section 2 that illustrates how the location of the coupling point can affect distortion in a quarter-car representation of a vehicle. Then, in Section 3.1, a frequency-domain distortion metric from the haptics literature is adopted within the ID-HIL framework. Using this metric, Section 3.2 investigates which coupling point characteristics lead to a low distortion, and relates distortion to a sensitivity function. Section 3.3 establishes the signal-dependence of distortion, and Section 3.4 discusses the effect of causality on distortion. Finally, in Section 4, the theory developed is applied to the illustrative quarter-car example, and conclusions are drawn in Section 5.

2   Motivating example

Consider the system shown in Figure 1. This is a quarter–car representation of a vehicle, where the masses m_1, m_2 and m_3, represent the unsprung, sprung, and driver masses, respectively, and the corresponding spring-damper pairs capture the tyre, suspension, and seat stiffness and damping properties. The figure also shows the two coupling point

candidates considered in this study, labelled as CP1 and CP2. The coupling variables at these coupling points and their causalities are explicitly shown in Figure 2. A constant time delay τ is considered in both directions of communication, leading to a round-trip time delay 2τ. The input is the road velocity input, and the output of interest is the displacement of the suspension. The parameter values of the system are given in Table 1 and are representative of a military vehicle (Ersal et al., 2009).

Figure 1 Example system with two locations as potential coupling points
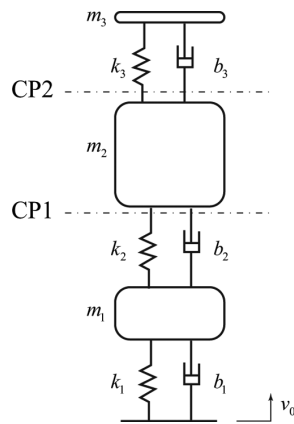

Figure 2 Subsystems and coupling causality shown explicitly for: (a) CP1 and (b) CP2
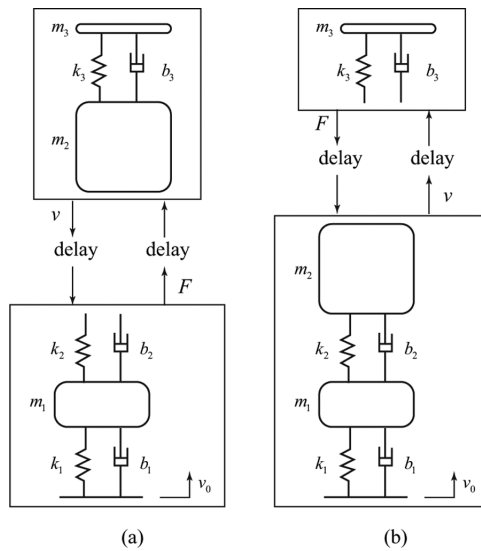

Figure 3 compares the unit step responses of the ideal system and the two systems in which the coupling variables at CP1 and CP2 are communicated with the constant time delay τ. As seen in the Figure, a delay at CP1 causes much more distortion than the same delay at CP2. This exemplifies the impact of the location of the coupling point on distortion and motivates the rest of the paper.

Table 1   Parameters of the example system

Parameter	Value
b_1	200 kNs/m
b_2	30 kNs/m
b_3	250 Ns/m
k_1	1 MN/m
K_2	275 kN/m
k_3	1.4 kN/m
m_1	110 kg
m_2	900 kg
m_3	20 kg
τ	20 ms

Figure 3   Comparing the unit step responses of the ideal system and the two systems with coupling points at CP1 and CP2 (see online version for colours)
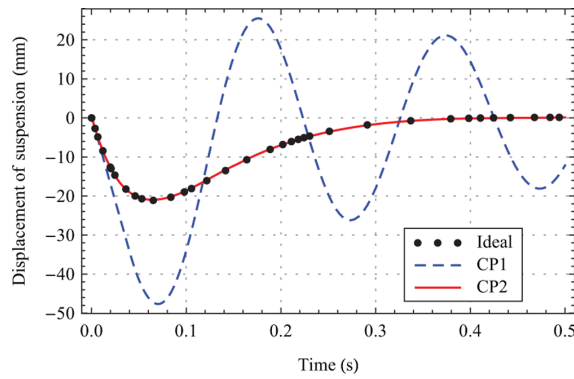
To justify the paper's focus on time delay only, the example system has also been simulated in an Internet-distributed manner using the communication framework reported in Ersal et al. (2012). The results of this simulation are shown in Figure 4 and, in addition to delay, include also the effects of jitter, loss, and distributed simulation. During this simulation, roundtrip time delay was observed to vary between 33 ms and 44 ms, with an average value of 38 ms. The drop rate of the network was found to be 0.07%. The coupling variables were communicated at a rate of 500 Hz, i.e., every 2 ms. The similarity between Figures 3 and 4 suggests that delay is indeed the dominant cause for distortion in this example. It is important to keep in mind, however, that this does not have to be true in every example (Ersal et al., 2012).

3   Coupling point analysis

3.1   A metric for distortion

Consider an ID-HILS system, which, for some choice of input and output variables, has an ideal reference transfer function R_d, which is the system transfer function without any

communication delays. Let the transfer function of this system in the presence of communication delay be P. Then, one can define a frequency domain distortion metric by subtracting R_d from P and normalising with respect to R_d, i.e.,

$$\Theta = \frac{P - R_d}{R_d}.$$

(1)

This definition of distortion was first introduced by Griffiths et al. within the haptics domain, where R_d represented the reference dynamics to be rendered to the user through a haptic device, and P represented the actual dynamics rendered to the user (Griffiths et al., 2008).

Figure 4 Internet-distributed simulation results of the example system (see online version for colours)
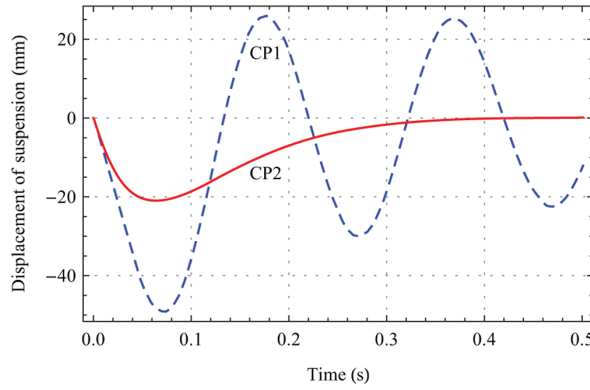
In the following discussion, an ID-HIL system is treated involving only two sites, a local site and a remote site. The reference dynamics R_d in this case are achieved through an ideal coupling (involving bilateral communications without delay) of the local and remote dynamics. Figure 5 depicts the reference dynamics in block diagram form, where G and G_r refer to the local and remote dynamics, respectively, u_1 is the external input to the local system, y_1 is the output of interest in the local system, and u_2 and y_2 are the coupling variables between the local and remote systems. Generally, the variables u_2 and y_2 are power-conjugate variables modelling an energetic connection, such as force and velocity in the mechanical domain, but this need not be true in every ID-HIL system. The reference system equations are given as

$$\begin{bmatrix} y_1 \\ y_2 \end{bmatrix} = \begin{bmatrix} G_{11} & G_{12} \\ G_{21} & G_{22} \end{bmatrix} \begin{bmatrix} u_1 \\ u_2 \end{bmatrix}$$
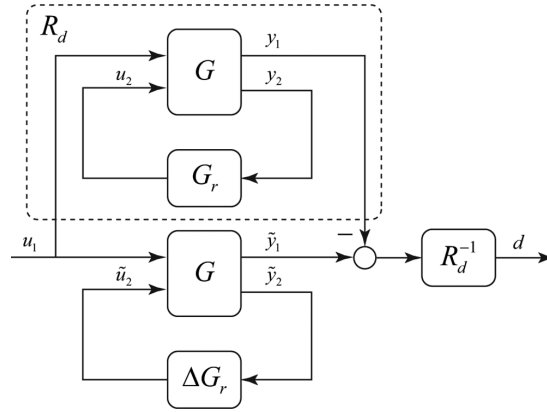
$$u_2 = G_r y_2$$

(2)

from which the reference dynamics R_d from u_1 to y_1 can be derived as

$$R_d = \frac{G_{11} + (G_{12}G_{21} - G_{11}G_{22})G_r}{1 - G_{22}G_r} = \frac{G_{11} + A}{1 - G_{22}G_r}$$

(3)

where $A = (G_{12}G_{21} - G_{11}G_{22})G_r$. Making the coupling point explicit enables an analysis of the effects of choosing different coupling points.

Figure 5   Expressing the reference dynamics in block diagram form
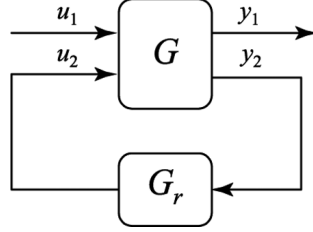
Next, to capture the effect of delay due to the introduction of Internet communications in an ID-HIL setup, consider a multiplicative perturbation Δ to the remote dynamics G_r. This multiplicative form is suitable for capturing the dynamics of Internet delay and could also capture other unmodelled dynamics such as the dynamics of the sensors and actuators. Figure 6 expresses the adoption of the distortion metric into the ID-HIL framework in block diagram form, where distortion is the transfer function from u_1 to d.

Figure 6   Adoption of the distortion metric into the ID-HIL framework

The actual system equations become

$$\begin{bmatrix} \tilde{y}_1 \\ \tilde{y}_2 \end{bmatrix} = \begin{bmatrix} G_{11} & G_{12} \\ G_{21} & G_{22} \end{bmatrix} \begin{bmatrix} u_1 \\ \tilde{u}_2 \end{bmatrix}$$

$$\tilde{u}_2 = \Delta G_r \tilde{y}_2$$

(4)

where tildes are used to differentiate the ideal variables from the actual variables. From equation (4), the actual dynamics P from u_1 to $\tilde{y}_1$ can be derived as

$$P = \frac{G_{11} + \Delta A}{1 - \Delta G_{22} G_r}$$

(5)

The distortion metric for the ID-HIL framework can then be found as

$$\Theta = \frac{P - R_d}{R_d} = \frac{G_{12} G_{21} G_r (\Delta - 1)}{(1 - \Delta G_{22} G_r)(G_{11} + A)}.$$

(6)

Equation (6) provides a means to analyse the impact on distortion of different coupling points in an ID-HIL system. Different coupling points will lead to different definitions of local and remote dynamics, i.e., different G_{12}, G_{21}, G_{11}, G_{22} and G_r, even though the delay dynamics and other perturbation factors lumped in Δ may remain invariant, which is assumed to be the case in this paper. Therefore, different coupling points will, in general, yield different distortion values, and equation (6) can quantify their impact on distortion.

3.2 Distortion analysis

In the framework created in Section 3.1, the ultimate goal of bringing the actual dynamics as close as possible to the reference dynamics translates to achieving a distortion that is as small as possible. Since distortion is a transfer function and thus a function of frequency, it is also possible to define frequency ranges over which the distortion is desired to be small.

Equation (6) reveals that there are a number of ways to achieve a small distortion at a given frequency. Specifically, besides the trivial case of $\Delta = 1$, i.e., no perturbation, the distortion will be small for a given frequency, if one of the following is true at that frequency:

1    $G_{11} \rightarrow \infty$: the input u_1 is greatly amplified at the output y_1 and thus the contribution through the coupling with the remote system is negligible

2    $G_{12} \rightarrow 0$: the feedback u_2 from the remote system has a very small effect on the output of interest y_1

3    $G_{21} \rightarrow 0$: the external input u_1 has a very small effect on the coupling variable y_2

4    $G_r \rightarrow 0$: the remote system does not affect the local system, i.e., it is driven by the local system without any impedance and the coupling is almost one-way

5    $G_r \rightarrow \infty$: the remote system has very high impedance

6    $G_{22} \rightarrow \infty$: the local impedance at the coupling point is very high.

Thus, to achieve low distortion, one can look for a coupling point that will lead to one of the conditions listed above. The physical interpretation associated with each condition can help in selecting coupling points by inspection. Such an ad hoc approach may be intuitively appealing, but will be difficult to apply in a systematic manner to complex real-life systems. Fortunately, one can summarise the above conditions using a single formal metric, namely, the sensitivity of the reference dynamics to the remote dynamics. A formal definition is given by

$$S_r := \frac{\partial R_d / R_d}{\partial G_r / G_r} \tag{7}$$

In words, it is defined as the ratio of a relative change in the reference dynamics to a relative change in the remote dynamics. Evaluation of S_r for the framework given in Figure 5 leads to

$$S_r = \frac{G_{12}G_{21}G_r}{(1-G_{22}G_r)(G_{11}+A)} \tag{8}$$

Comparing equations (6) and (8), the following relationship between distortion and sensitivity to remote dynamics can be derived:

$$\Theta = S_r \frac{1-G_{22}G_r}{1-\Delta G_{22}G_r}(\Delta-1) \tag{9}$$

From equation (9) it can be seen that distortion will be small when the sensitivity to remote dynamics is small, and it can be easily verified that the conditions listed previously are also the conditions under which S_r becomes small. Hence, S_r provides a unifying concept for those conditions and also a single intuitive, physical explanation for distortion.

Furthermore, expanding the expression for distortion in equation (6) in a Taylor series around $\Delta = 1$ shows that, to a first order approximation, distortion is given by $S_r (\Delta - 1)$, i.e.,

$$\Theta = S_r(\Delta-1)+O((\Delta-1)^2) \tag{10}$$

Thus, to a first order approximation, and recalling that Δ is assumed to be invariant to the location of the coupling point, the difference in distortion caused by different coupling points is completely captured by the sensitivity function S_r. The significance of this finding can be seen by referring to equation (8) and noting that S_r can be evaluated without knowledge of the perturbation Δ. Therefore, S_r not only provides a single metric to be considered when comparing coupling points, but also this metric, unlike Θ itself, is independent of Δ. This allows for comparing coupling points without having to define an expression for Δ.

Equation (10) further implies that

$$S_r = \frac{\partial R_d / R_d}{\partial G_r / G_r} = \frac{\partial \Theta}{\partial \Delta}\bigg|_{\Delta=1} \tag{11}$$

That is, the sensitivity S_r is the gradient of the distortion metric with respect to the perturbation Δ at $\Delta = 1$, i.e., the case when there is no perturbation.

Having related S_r to Θ, we can now go back to equation (7) to explain how a coupling point can be selected. Distortion will be small if a relative change in the remote dynamics creates a small relative change in the reference dynamics. Thus, the task of finding the best coupling point now translates to finding the coupling point that partitions into G_r all the dynamics whose relative change affects the reference system dynamics the least.

3.3   On the signal dependence of distortion

It is important to note that distortion is defined for a particular output of interest y_1. Even though the formulation allows y_1 to be any signal in the local system, a low distortion in y_1 does not necessarily imply that the distortion will be low in all signals in the local system. This is easily demonstrated by considering the distortions in y_1 and y_2 simultaneously.

Following the same steps as for y_1, the distortion in y_2 can be derived as

$$\Theta_{y_2} = \frac{G_{22}G_r(\Delta-1)}{1-\Delta G_{22}G_r} \qquad (12)$$

Thus, it can be seen that, besides the trivial condition $\Delta\to1$ (i.e., no perturbation), there is only one condition under which both Θ and Θ_{y_2} become small, namely, $G_r\to0$. The conditions 1, 2, 3, 5, and 6 do not necessarily imply a small Θ_{y_2}, and the condition $G_{22}\to0$, which makes Θ_{y_2} small, does not necessarily make Θ small. This emphasises the fact that distortion is not an independent property of the system, but is output-signal dependent, as observed experimentally before (Ersal et al., 2012). Therefore, when analysing distortion, it is important to keep in mind the signals with respect to which distortion is defined.

3.4 On the effect of causality on distortion

Under some conditions, distortion can be improved simply by changing input-output causality. Consider the case where $G_{22}\to0$. Furthermore, assume that G_{22}^{-1} and G_r^{-1} are proper. In this case, a switch in causality as shown in Figure 7 leads to the following ideal system equations

$$\begin{bmatrix} y_1 \\ u_2 \end{bmatrix} = \begin{bmatrix} G_{11} & G_{12}G_{22}^{-1} \\ -G_{21}G_{22}^{-1} & G_{22}^{-1} \end{bmatrix}\begin{bmatrix} u_1 \\ y_2 \end{bmatrix}$$
$$y_2 = G_r^{-1}u_2 \qquad (13)$$

that gives

$$R_d^* = \frac{G_{12}G_{21} + G_{11}G_{22}(1-G_{22}G_r)}{G_{22}(1-G_{22}G_r)} \qquad (14)$$

where the asterisk is used to denote the switched-causality case. Assuming a multiplicative perturbation Δ as before leads to

$$P^* = \frac{\Delta G_{12}G_{21} + G_{11}G_{22}(\Delta-G_{22}G_r)}{G_{22}(\Delta-G_{22}G_r)}. \qquad (15)$$

Finally, the expression for distortion is obtained as

$$\Theta^* = \frac{P^* - R_d^*}{R_d^*}$$
$$= \frac{(1-\Delta)G_{12}G_{21}G_{22}G_r}{(\Delta-G_{22}G_r)(G_{12}G_{21} + G_{11}G_{22}(1-G_{22}G_r))}. \qquad (16)$$

From equation (16) it can be seen that

$$\lim_{G_{22}\to0} \Theta^* = 0. \qquad (17)$$

Thus, distortion is reduced by switching the causality at the coupling point. Note that this may only be feasible for certain ID-HILS configurations, i.e., those with proper G_{22}^{-1} and G_r^{-1}.

Figure 7 Switching causality at the coupling point
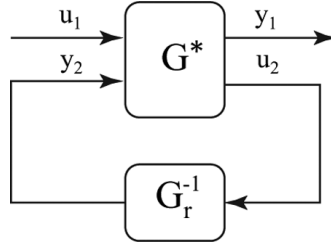
4 Application to the example

In this section, the theory that is presented in Section 3 is applied to the quarter-car example that was introduced in Section 2 for illustration purposes.

The system equations can be written and put into the framework described in Section 3 as follows. From Figure 2, the system and output equations for the local system can be derived in the Laplace domain as:

$$m_1 s^2 x_1 = -F_{k1} - F_{b1} + F_{k2} + F_{b2}$$
$$d_{k2} = x_2 - x_1 \tag{18}$$
$$F = F_{k2} + F_{b2}$$

with

$$F_{k1} = k_1(x_1 - x_0)$$
$$F_{k2} = k_2(x_2 - x_1)$$
$$F_{b1} = b_1 s(x_1 - x_0)$$
$$F_{b2} = b_2 s(x_2 - x_1) \tag{19}$$
$$x_2 = \frac{1}{s}v$$
$$x_0 = \frac{1}{s}v_0$$

and x_1 referring to the position of mass m_1. The system and output equations for the remote system are

$$m_2 s^2 x_2 = -F + F_{k3} + F_{b3}$$
$$m_3 s^2 x_3 = -F_{k3} - F_{b3} \tag{20}$$
$$v = sx_2$$

with

$$F_{k3} = k_3(x_3 - x_2)$$
$$F_{b3} = b_3 s(x_3 - x_2)$$
(21)

and x_2 and x_3 referring to the positions of masses m_2 and m_3, respectively. Equations (18)–(21) for CP1 can be put into the framework shown in Figure 5 as:

$$G_{11} = \frac{d_{k2}}{v_0} = \frac{-(b_1 s + k_1)}{s(m_1 s^2 + (b_1 + b_2)s + k_1 + k_2)}$$

$$G_{12} = \frac{d_{k2}}{v} = \frac{m_1 s^2 + b_1 s + k_1}{s(m_1 s^2 + (b_1 + b_2)s + k_1 + k_2)}$$

$$G_{21} = \frac{F}{v_0} = \frac{-(b_1 s + k_1)(b_2 s + k_2)}{s(m_1 s^2 + (b_1 + b_2)s + k_1 + k_2)}$$
(22)

$$G_{22} = \frac{F}{v} = \frac{(b_2 s + k_2)(m_1 s^2 + b_1 s + k_1)}{s(m_1 s^2 + (b_1 + b_2)s + k_1 + k_2)}$$

$$G_r = \frac{v}{F} = \frac{-(m_3 s^2 + b_3 s + k_3)}{s(m_2 m_3 s^2 + b_3(m_2 + m_3)s + k_3(m_2 + m_3))}.$$

Similarly, for CP2, the system and output equations for the local system can be derived as:

$$m_1 s^2 x_1 = -F_{k1} - F_{b1} + F_{k2} + F_{b2}$$
$$m_2 s^2 x_2 = -F_{k2} - F_{b2} + F$$
$$d_{k2} = x_2 - x_1$$
$$v = s x_2.$$
(23)

The system and output equations for the remote system are

$$m_3 s^2 x_3 = -F_{k3} - F_{b3}$$
$$F = F_{k3} + F_{b3}.$$
(24)

From equations (23) and (24), the G_{ij} and G_r terms can be derived as

$$G_{11} = \frac{d_{k2}}{v_0} = \frac{-m_2 s(b_1 s + k_1)}{D}$$

$$G_{12} = \frac{d_{k2}}{F} = \frac{m_1 s^2 + b_1 s + k_1}{D}$$

$$G_{21} = \frac{v}{v_0} = \frac{(b_1 s + k_1)(b_2 s + k_2)}{D}$$
(25)

$$G_{22} = \frac{v}{F} = \frac{s(m_1 s^2 + (b_1 + b_2)s + k_1 + k_2)}{D}$$

$$G_r = \frac{F}{v} = \frac{-m_3 s(b_3 s + k_3)}{m_3 s^2 + b_3 s + k_3}$$

with

$$D = m_2 s^2 (m_1 s^2 + (b_1 + b_2)s + k_1 + k_2)$$
$$+(b_2 s + k_2)(m_1 s^2 + b_1 s + k_1). \tag{26}$$

For both coupling points, we have:

$$\Delta = e^{-2\tau s}. \tag{27}$$

An analysis of distortion using the proposed framework provides a frequency domain explanation to the different performance levels observed with the two coupling points for the same delay conditions. Figure 8 compares the distortion metric for the two coupling points. As the figure shows, the distortion for the system with CP2 is much less than the distortion for the system with CP1 at all frequencies, and hence, CP2 is a better choice of coupling point than CP1. The fact that distortion peaks to about 20 dB around 30 rad/s for CP1 is likely the dominant reason for the oscillations observed in the CP1 response in Figure 3. Specifically, 20 dB distortion magnitude indicates that the steady-state magnitude error due to delay at CP1 will be 10 times the reference magnitude. Moreover, the frequency of about 30 rad/s where the peak occurs corresponds directly to the period of the oscillations in Figure 3, which is about 0.2 s. On the other hand, the close agreement between the ideal system and the system with CP2 is due to the fact that the magnitude of distortion is below approximately –40 dB at all frequencies for CP2. It is important to stress however, that distortion is a frequency dependent metric, and one coupling point may not always stand out as the better choice for all frequencies as in this example.

Figure 8   The magnitude of the distortion metric for the two coupling points CP1 and CP2 (see online version for colours)
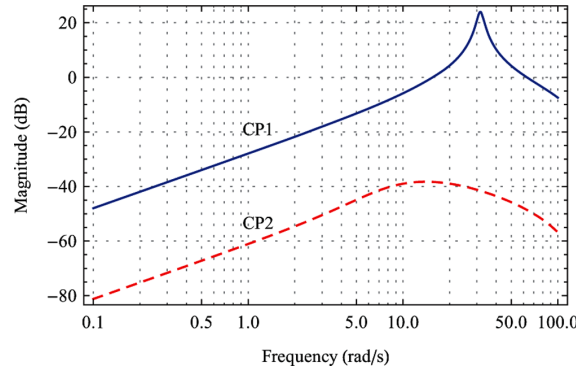
To gain more physical insight, Figure 9 compares the sensitivity, S_r, of the reference dynamics to the remote dynamics for the two coupling points CP1 and CP2. The sensitivity S_r is less for CP2 than CP1 for all frequencies, explaining why the distortion with CP2 is lower relative to the distortion with CP1.

Figure 10 further reveals in more detail why the sensitivity S_r, and thus distortion, is low for CP2 by showing the magnitudes of the transfer functions G_{ij}, $i, j = 1, 2$, and G_r. Specifically, the distortion is low due to the fact that G_{12} remains small across the entire frequency range. Physically, this corresponds to the fact that the driver and seat subsystem has a very small effect on the rest of the vehicle, because the reaction forces of the driver and seat subsystem have only a small effect on the sprung mass, which

is the largest mass in the system. When this sprung mass is considered as part of the remote system, as is the case with CP1, the sensitivity of the reference dynamics to the remote system increases, which explains the higher sensitivity and distortion observed for CP1. This observation may look counterintuitive when condition 5 in Section 3.2 is considered, because one may initially expect CP1 to be a good choice, too, since placing the largest mass in the system into G_r would increase the inertia of the remote system and help increase its impedance. However, the analysis shows that the sprung mass is not large enough to have sufficient impedance relative to the local system for distortion attenuation, and the disadvantage of losing the inertia in the local system clearly offsets the benefits of increasing the inertia of the remote system.

Finally, Figure 11 shows the magnitude plot of G_{22} for CP1. The magnitude being significantly greater than zero implies that distortion cannot be improved by reversing the causality at CP1. Thus, improving distortion for CP1 requires other methods such as feedback and/or feed forward control (Horiuchi et al., 1999; Blakeborough et al., 2001; Darby et al., 2002; Wallace et al., 2005; Jung and Shing, 2006; Wagg et al., 2008). Development of such methods, however, is beyond the scope of this paper.

Figure 9 The magnitude of sensitivity of the reference dynamics to the remote dynamics for the two coupling points CP1 and CP2 (see online version for colours)
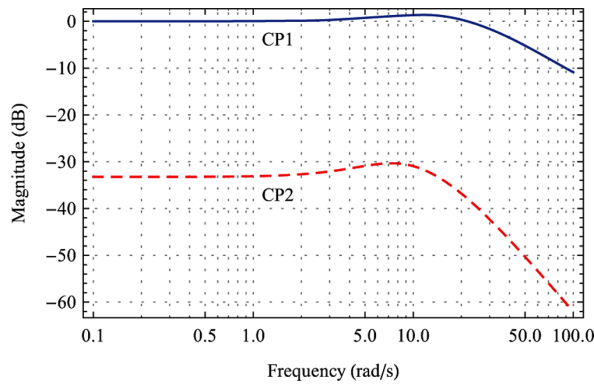

Figure 10 The magnitude of G_{ij}, $i, j = 1,2$, and G_r for CP2 as factors affecting sensitivity S_r (see online version for colours)
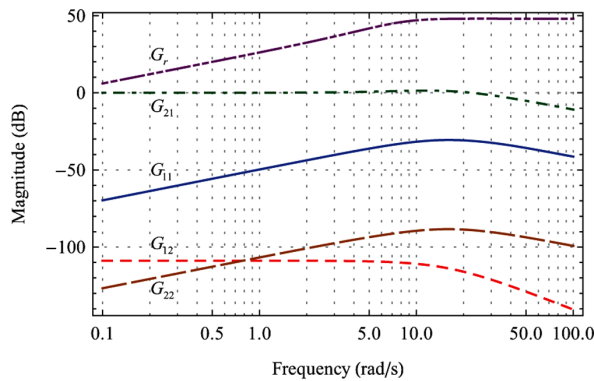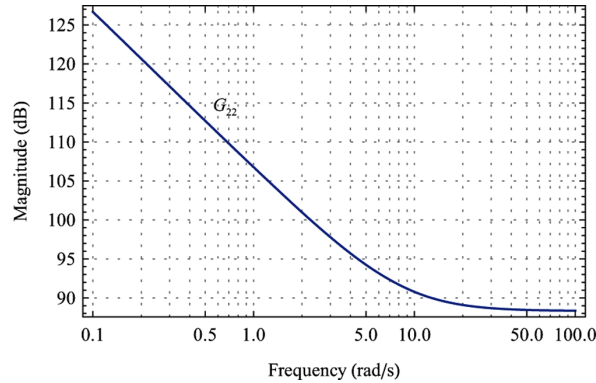
Figure 11 The magnitude of G_{22} for CP1 (see online version for colours)

5   Summary and conclusion

The original contributions of this paper can be summarised as follows. This paper considers the coupling point as a design variable in ID-HILS systems and proposes a framework for a frequency-domain analysis of the impact of the coupling point location on distortion. A distortion metric from the haptics literature is adopted into this framework. Using this framework and metric, the paper identifies the system characteristics that render a coupling point location suitable for ID-HILS in the sense that it leads to a low distortion. The paper further identifies the sensitivity of the reference dynamics to the dynamics of the remote system as the unifying reason for different distortion results obtained with different coupling points. It also shows that distortion is an output-signal dependent concept and can, in some cases, be affected not only by the location of the coupling point, but also by the coupling causality. The paper applies this theory to a quarter-car model to illustrate and explain the differences between two coupling points. The proposed theory is found useful when delay is the dominant cause of distortion in an Internet-distributed simulation.

References

Aghili, F. and Piedboeuf, J-C. (2002) 'Contact dynamics emulation for hardware-in-loop simulation of robots interacting with environment', *IEEE International Conference on Robotics and Automation*, IEEE Washington, D.C, Vol. 1, pp.523–529.

Anderson, R.J. and Spong, M.W. (1989) 'Bilateral control of teleoperators with time delay', *IEEE Transactions on Automatic Control*, Vol. 34, No. 5, pp.494–501.

Bacic, M., Neild, S. and Gawthrop, P. (2009) 'Introduction to the special issue on hardware-in-the-loop simulation', *Mechatronics*, Vol. 19, No. 7, pp.1041, 1042.

Blakeborough, A., Williams, M.S., Darby, A.P. and Williams, D.M. (2001) 'The development of real-time substructure testing', *Philosophical Transactions of the Royal Society of London Series a-Mathematical Physical and Engineering Sciences*, Vol. 359, Nos. 1786, pp.1869–1891.

Brudnak, M., Pozolo, M., Paul, V., Mohammad, S., Smith, W., Compere, M., Goodell, J., Holtz, D., Mortsfield, T. and Shvartsman, A. (2007) 'Soldier/Harware-in-the-loop simulation-based combat vehicle duty cycle measurement: duty cycle experiment 2', *Simulation*

Interoperability Workshop, Norfolk, VA, Simulation Interoperability Standards Organisation (SISO), Norfolk, VA, pp.7–16.

Buford Jr, J.A., Jolly, A.C. Mobley, S.B. and Sholes, W.J. (2000) 'Advancements in hardware-in-the-loop simulations at the U.S. Army Aviation and Missile Command', *SPIE – Technologies for Synthetic Environments: Hardware-in-the-Loop Testing V*, SPIE.

Cai, G., Chen, B.M., Lee, T.H. and Dong, M. (2009) 'Design and implementation of a hardware-in-the-loop simulation system for small-scale UAV helicopters', *Mechatronics*, Vol. 19, No. 7, pp.1057–1066.

Çavuşoğlu, M.C., Sherman, A. and Tendick, F. (2002) 'Design of bilateral teleoperation controllers for haptic exploration and telemanipulation of soft environments', *IEEE Transactions on Robotics and Automation*, Vol. 18, No. 4, pp.641–647.

Compere, M., Goodell, J. Simon, M. Smith, W. and Brudnak, M. (2006) *Robust Control Techniques Enabling Duty Cycle Experiments Utilising a 6-Dof Crewstation Motion Base, A Full Scale Combat Hybrid Electric Power System, and Long Distance Internet Communications*, SAE Technical Paper, Number: 2006-01-3077.

Darby, A.P., Williams, M.S. and Blakeborough, A. (2002) 'Stability and delay compensation for real-time substructure testing', *Journal of Engineering Mechanics*, Vol. 128, No. 12, pp.1276–1284.

De Gersem, G., Van Brussel, H. and Tendick, F. (2005) 'Reliable and enhanced stiffness perception in soft-tissue telemanipulation', *International Journal of Robotics Research*, Vol. 24, No. 10, pp.805–822.

Elhajj, I., Ning, X. Wai Keung, F. Yun-Hui, L. Hasegawa, Y. and Fukuda, T. (2003) 'Supermedia-enhanced Internet-based telerobotics', *Proceedings of the IEEE*, Vol. 91, No. 3, pp.396–421.

Ersal, T., Brudnak, M., Salvi, A., Stein, J.L., Filipi, Z. and Fathy, H.K. (2011) 'Development and model-based transparency analysis of an Internet-distributed hardware-in-the-loop simulation platform', *Mechatronics*, Vol. 21, No. 1, pp.22–29.

Ersal, T., Brudnak, M., Stein, J.L. and Fathy, H.K. (2012) 'Statistical transparency analysis in Internet-distributed hardware-in-the-loop simulation', *IEEE/ASME Transactions on Mechatronics*. Vol. 17, No. 2, pp.228–238.

Ersal, T., Kittirungsi, B., Fathy, H.K. and Stein, J.L. (2009) 'Model reduction in vehicle dynamics using importance analysis', *Vehicle System Dynamics*, Vol. 47, No. 7, pp.851–865.

Fathy, H.K., Filipi, Z.S., Hagena, J. and Stein, J.L. (2006) 'Review of hardware-in-the-loop simulation and its prospects in the automotive area', *SPIE – Modeling and Simulation for Military Applications*, Kissimmee, FL, USA, SPIE.

Ganguli, A., Deraemaeker, A., Horodinca, M. and Preumont, A. (2005) 'Active damping of chatter in machine tools – demonstration with a 'hardware-in-the-loop' simulator', *Journal of Systems and Control Engineering*, Vol. 219, No. 5, pp.359–369.

Gawthrop, P.J., Neild, S.A., Gonzalez-Buelga, A. and Wagg, D.J. (2009) 'Causality in real-time dynamic substructure testing', *Mechatronics*, Vol. 19, No. 7, pp.1105–1115.

Goodell, J., Compere, M., Simon, M., Smith, W., Wright, R. and Brudnak, M. (2006) *Robust Control Techniques for State Tracking in the Presence of Variable Time Delays*, SAE Technical Paper, Number: 2006-01-1163.

Griffiths, P.G., Gillespie, R.B. and Freudenberg, J.S. (2008) 'A fundamental tradeoff between performance and sensitivity within haptic rendering', *IEEE Transactions on Robotics*, Vol. 24, No. 3, pp.537–548.

Horiuchi, T., Inoue, M. Konno, T. and Namita, Y. (1999) 'Real-time hybrid experimental system with actuator delay compensation and its application to a piping system with energy absorber', *Earthquake Engineering and Structural Dynamics*, Vol. 28, No. 10, pp.1121–1141.

Huber Jr, E.G. and Courtney, R.A. (1997) 'Hardware-in-the-loop simulation at Wright Laboratory's Dynamic Infrared Missile Evaluator (DIME) facility', *Technologies for Synthetic Environments: Hardware-in-the-Loop Testing II*, SPIE.

Jung, R-Y. and Shing, P.B. (2006) 'Performance evaluation of a real-time pseudodynamic test system', *Earthquake Engineering and Structural Dynamics*, Vol. 35, No. 7, pp. 789–810.

Kelf, M.A. (2001) 'Hardware-in-the-loop simulation for undersea vehicle applications', *SPIE – Technologies for Synthetic Environments: Hardware-in-the-Loop Testing VI*, SPIE.

Kimura, A. and Maeda, I. (1996) 'Development of engine control system using real time simulator', *IEEE International Symposium on Computer-Aided Control System Design*, pp.157–163.

Lawrence, D.A. (1993) 'Stability and transparency in bilateral teleoperation', *IEEE Transactions on Robotics and Automation*, Vol. 9, No. 5, pp.624–637.

Lee, D. and Spong, M.W. (2006) 'Passive bilateral teleoperation with constant time delay', *IEEE Transactions on Robotics*, Vol. 22, No. 2, pp.269–281.

Leitner, J. (2001) 'A hardware-in-the-loop testbed for spacecraft formation flying applications', *IEEE Aerospace Conference*, IEEE, Vol. 2, pp.615–620.

Mahin, S., Nigbor, R., Pancake, C., Reitherman, R. and Wood, S. (2003) 'The establishment of the NEES consortium', *ASCE/SEI Structures Congress and Exposition: Engineering Smarter*, American Society of Civil Engineers, pp.181–182.

Mosqueda, G., Stojadinovic, B., Hanley, J., Sivaselvan, M. and Reinhorn, A.M. (2008) 'Hybrid seismic response simulation on a geographically distributed bridge model', *Journal of Structural Engineering*, Vol. 134, No. 4, pp.535–543.

Niemeyer, G. and Slotine, J-J.E. (1991) 'Stable adaptive teleoperation', *IEEE Journal of Oceanic Engineering*, Vol. 16, No. 1, pp.152–162.

Niemeyer, G. and Slotine, J-J.E. (2002) 'Toward bilateral Internet teleoperation', *In Beyond webcams: an introduction to online robots*, MIT Press, pp.193–213.

Pan, P., Tada, M. and Nakashima, M. (2005) 'Online hybrid test by internet linkage of distributed test-analysis domains', *Earthquake Engineering and Structural Dynamics*, Vol. 34, No. 11, pp.1407–1425.

Spencer, B.F., Elnashai, A., Nakata, N., Saliem, H., Yang, G., Futrelle, J., Glick, W., Marcusiu, D., Ricker, K., Finholt, T., Horn, D., Hubbard, P., Keahey, K., Liming, L., Zaluzec, N., Pearlman, L. and Stauffer, E. (2004) The MOST Experiment: Earthquake Engineering on the Grid, NEESgrid, Technical Report NEESgrid-2004-41.

Stojadinovic, B., Mosqueda, G. and Mahin, S.A. (2006) 'Event-driven control system for geographically distributed hybrid simulation', *Journal of Structural Engineering*, Vol. 132, No. 1, pp.68–77.

Tsai, K-C., Yeh, C-C., Yang, Y-S., Wang, K-J., Wang, S-J. and Chen, P-C. (2003) 'Seismic hazard mitigation: Internet-based hybrid testing framework and examples', *International Colloquium on Natural Hazard Mitigation: Methods and Applications*, France.

Verma, R., Del Vecchio, D. and Fathy, H.K. (2008) 'Development of a scaled vehicle with longitudinal dynamics of an HMMWV for an ITS testbed', *IEEE/ASME Transactions on Mechatronics*, Vol. 13, No. 1, pp.46–57.

Wagg, D., Neild, S. and Gawthrop, P. (2008) 'Real-time testing with dynamic substructuring', in Bursi, O.S. and Wagg, D. (Eds.): *Modern Testing Techniques for Structural Systems*. Springer, Italy, pp.293–342.

Wallace, M., Sieber, I.J., Neild, S.A., Wagg, D.J. and Krauskopf, B. (2005) 'Stability analysis of real-time dynamic substructuring using delay differential equation models', *Earthquake Engineering and Structural Dynamics*, Vol. 34, No. 15, pp.1817–1832.

Watanabe, E., Kitada, T. Kunitomo, S. and Nagata, K. (2001) 'Parallel pseudodynamic seismic loading test on elevated bridge system through the internet', *8th East Asia-Pacific Conference on Structural Engineering and Construction*, Singapore.

White, G.D., Bhatt, R.M., Tang, C.P. and Krovi, V.N. (2009) 'Experimental evaluation of dynamic redundancy resolution in a nonholonomic wheeled mobile manipulator', *IEEE/ASME Transactions on Mechatronics*, Vol. 14, No. 3, pp.349–357.

Xi, N. and Tarn, T.J. (2000) 'Stability analysis of non-time referenced Internet-based telerobotic systems', *Robotics and Autonomous Systems*, Vol. 32, No. 2, pp.173–178.

Yokokohji, Y. and Yoshikawa, T. (1994) 'Bilateral control of master-slave manipulators for ideal kinesthetic coupling – formulation and experiment', *IEEE Transactions on Robotics and Automation*, Vol. 10, No. 5, pp.605–619.

Yue, X., Vilathgamuwa, D.M. and Tseng, K-J. (2005) 'Robust adaptive control of a three-axis motion simulator with state observers', *IEEE/ASME Transactions on Mechatronics*, Vol. 10, No. 4, pp.437–448.

Zhang, R. and Alleyne, A.G. (2005) 'Dynamic emulation using an indirect control input', *Journal of Dynamic Systems, Measurement and Control*, Vol. 127, No. 1, pp.114–124.

Nomenclature

b	Damping coefficient
Δ	Multiplicative perturbation
F, F_b, F_k	Coupling, damping, and spring forces
G, G_r	Local and remote plant dynamics
k	Spring stiffness
m	Mass
P	System dynamics including delay at coupling point
Θ	Distortion
R_d	Reference system dynamics
s	Laplace variable
S_r	Sensitivity of the reference dynamics to the remote dynamics
τ	Time delay
u_1, u_2	System inputs
v, v_0	Coupling and input velocities
$x\,x$	Position
y_1, y_2	Desired system outputs
$\tilde{y}_1, \tilde{y}_2$	Actual system outputs